Uludağ University Journal of The Faculty of Engineering, Vol. 23, No. 2, 2018 RESEARCH

DOI: 10.17482/uumfd.470660

EFFECT OF ATTACK ANGLE ON FLOW AROUND A SQUARE PRISM WITH A SPLITTER PLATE

Mehmet SEYHAN [*]
Mustafa SARIOĞLU [*]
Yahya Erkan AKANSU [**]

Alınma:25.09.2016; düzeltme:01.12.2017; kabul:22.06.2018

Abstract: Lift and drag forces on a square prism with a (splitter) plate are experimentally investigated by force measurements with a load cell. Results showed that drag and lift coefficients are independent of Reynolds number for Re = 9700 – 36500 at 0°, 45°, 90°, 135° and 180°. Drag coefficient at 0° is obtained as 2.02 for the square prism alone, and 1.04 for the square cylinder with splitter plate. Maximum drag reduction for the square cylinder with the plate is 50% as compared to the square cylinder at 0° and 15°. For $\alpha < 30°$ and $\alpha > 114°$, drag coefficient of a square prism with splitter plate is smaller than that of the square prism alone. At Re = 20000, lift and drag coefficients significantly change with increasing attack angle.

Keywords: Square prism; Splitter plate; Drag coefficient; Lift coefficient.

Ayırıcı Plakalı Bir Kare Prizma Etrafındaki Akışta Hücum Açısının Etkisi

Öz: Farklı hücum açılarında akış ayırıcı plakalı bir kare prizmaya etki eden kaldırma ve sürükleme kuvvetleri yük hücresiyle ölçülerek deneysel olarak incelenmiştir. Sonuçlar, kaldırma ve sürükleme katsayılarının Re = 9700 – 36500 aralığında 0°, 45°, 90°, 135° ve 180° hücum açıları için Reynolds sayısından bağımsız olduğunu göstermiştir. Sürükleme katsayısı 0° hücum açısında tek kare prizma için 2.02 ve ayırıcı plakalı kare durumunda ise 1.04 olarak elde edilmiştir. Plakalı kare için maksimum sürükleme katsayısındaki azalma 50% olarak 0° ve 15°'de elde edilmiştir. $\alpha <30°$ ve $\alpha >114°$ aralıkları için, plakalı karenin sürükleme katsayısı sade karenin sürükleme katsayısından küçüktür. Re = 20000'de, kaldırma ve sürükleme katsayılarının önemli derecede hücum açısına bağlı olarak değiştiği görülmüştür.

Anahtar Kelimeler: Kare prizma, Ayırıcı plaka, Sürükleme katsayısı, Kaldırma katsayısı

[*] Karadeniz Technical University Engineering Faculty Mechanical Engineering, 61080, Trabzon.
[**] Niğde Ömer Halisdemir University Engineering Faculty Mechanical Engineering, 51240, Niğde

Corresponding Author: Mehmet SEYHAN (mehmetseyhan@ktu.edu.tr)

1. INTRODUCTION

Buff bodies such as circular and square cylinders are encountered in many engineering application including bridges, skyscrapers, electric poles, cooling towers, heat exchangers, truck-trailer and chimneys. Therefore, numerous researchers have tried to control the flow around basic bluff bodies in order to suppress/eliminate the fluctuating forces, flow separation and vortex shedding. Flow control methods are divided into two groups: the first one is active flow control (AFC) which relies on an external energy source and the second one is passive flow control (PFC) which is usually achieved by geometric modification of the body or addition of external geometries to the body. A moving surface (Zhang et al. 2010), a dielectric barrier discharge actuator (Akansu et al. 2013; Akbıyık et al. 2016), suction and blowing (Li et al. 2003), a vortex generator (Volino and Ibrahim 2012) and a piston cylinder mechanism (Gilarranz et al. 2005) can be given as examples of AFC methods. Splitter plates (Akansu et al. 2004; Sarioglu et al. 2006), passive vortex generators (Godard and Stanislas 2006) control rod (Akansu et al. 2011; Fırat et al. 2015; Sarioglu et al. 2005) and dimples (Bearman and Harvey 1993) can be listed as examples of PFC methods.

Sarioglu et al. (2006) studied the influence of adding a plate to a square prism with ratio L/D=1. In their study, the square prism with the plate is rotated from 0° to 180° at Re = 20000. To obtain the vortex shedding frequency, velocity measurement is performed by using a hot wire anemometer, while C_L and C_D are calculated from pressure measurements. They also indicated that the Strouhal number (St) is independent from Re = 7500 - 55000 and that the flow structure changes with varying attack angle. At 0°, 25% drag reduction is obtained as compared with the bare circular cylinder. Sarioglu (2017) performed an experimental study on the influence of a stationary splitter plate placed behind a square cylinder while rotating the object from 0° to 45° at Re = 30000. Pressure and velocity measurements were carried out. The results indicated that while minimum drag is obtained at 13°, there is an sudden increase in St at the same angle. Mansingh and Oosthuizen (1990) investigated the effects of splitter plates located behind a rectangular prism for Reynolds numbers between 3500 and 11500. Their results showed that vortex shedding frequency decreases and drag reduction is obtained up to 50% with the help of the splitter plate because of the increment of base pressure. Rathakrishnan (1999) researched the effect of a splitter plate, having six different splitter plate lengths, on the rear of a rectangular cylinder in the range 58000 < Re < 98000 in the wind tunnel. The rectangular prism together with a plate decreased C_D. This is due to the increment in the base pressure.

The purpose of the present study is to research the differences between force measurement and force calculated from pressure measurements with respect to Sarioglu et al. (2006). In this current study, the effect of the splitter plate placed behind a square cylinder is investigated experimentally. The drag and lift forces acting on this model are measured with the help of a load cell at attack angles from 0° to 180°. In order to reveal Reynolds independent, force measurement experiments are also carried out at a range of Reynolds numbers varying from 9700 to 36500 at 0°, 45°, 90°, 135° and 180°.

2. EXPERIMENTAL SETUP AND MEASUREMENT TECHNIQUES

An open and suction type wind tunnel having a square test section of 57 cm x 57 cm is used in these experiments (Fig. 1(a)). The closed test chamber having a length of 100 cm has a divergence angle of 0.3° and is made from transparent Plexiglas. Free stream velocity can be adjusted by using a frequency inverter and the turbulence intensity is smaller than 1%.

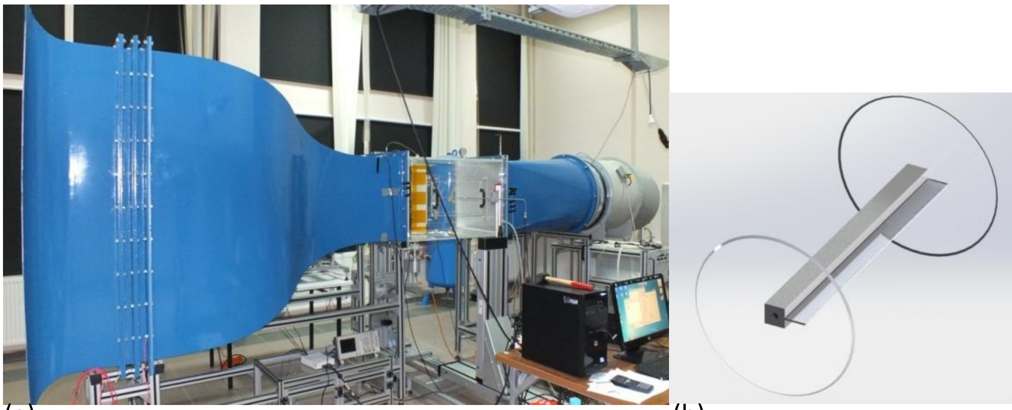

(a) **_Figure1:_** (b)

(a) General view of the wind tunnel and (b) schematic view of the test model

As illustrated in Figure 2, the experimental setup consists of a square prism, a splitter plate, two end plates, a rotary unit, a load cell and a connection rod. The square cylinder has an edge length of 40 mm and the end plates have a diameter of 280 mm and a thickness of 3 mm. The test model is assembled as shown in Fig. 1 (b). The spanwise width of the square prism placed between the end plates is 40 cm. The end plates are beveled at an angle of 45°. The blockage ratio of the square cylinder with splitter plate in the test section is equal to 4.9% at an angle of 0°. The square cylinder was placed at a distance of 20 cm from the inlet of the test section and placed in the middle of the chamber. An ISEL ZD30 rotary unit is used to rotate the test model clockwise between β=0° and 180° with 3° increments. A six axis ATI Gamma DAQ F/T load cell is placed on the rotary unit to measure aerodynamic forces. 10000 data are collected with a NI PCIe-6323 DAQ card at 0.5 kHz sampling frequency. The load cell can measure forces up to ±32 N at the direction of x and y axis. A ManoAir 500 model micromanometer and a pitot static tube were used to measure the free stream velocity (U_∞).

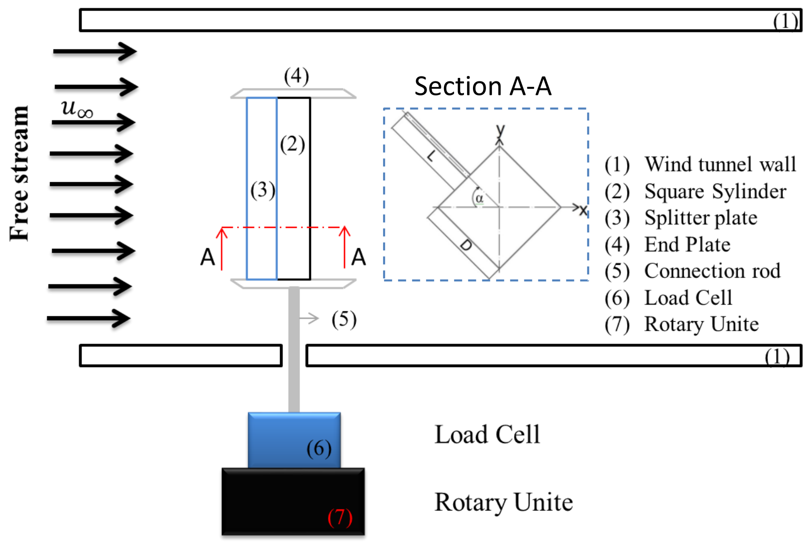

Figure2:

Schematic view of the experimental setup

Uncertainty analysis method is described in Eq.(1) by Coleman and Steele (2009).

$$u_r = \left[a^2\left(\frac{u_{x_1}}{X_1}\right)^2 + b^2\left(\frac{u_{x_2}}{X_2}\right)^2 + c^2\left(\frac{u_{x_3}}{X_3}\right)^2 + \cdots\right]^{1/2} \quad (1)$$

Uncertainty of the drag coefficient can be expressed in Eq. (2) like in the study of Bayındırlı (2017) and Akansu et al. (2016) by editing Eq. (1).

$$u_{C_D} = \frac{w_{C_D}}{C_D} = \left[(1)^2\left(\frac{w_{F_D}}{F_D}\right)^2 + (-1)^2\left(\frac{w_\rho}{\rho}\right)^2 + (-2)^2\left(\frac{w_{U\infty}}{U_\infty}\right)^2 + (-1)^2\left(\frac{w_A}{A}\right)^2\right]^{1/2} \qquad (2)$$

Here, u_{C_D} is the total uncertainty of the drag coefficient, C_D and F_D are the drag coefficient and drag force, w is the deviation, ρ is the air density, u_∞ is the free stream velocity and A is the frontal area of the truck trailer model. For Re = 20000, uncertainty of the drag coefficient is calculated as 6%. Similarly, the uncertainty of C_L is found to be 6.3%.

3. RESULTS AND DISCUSSION

A square cylinder with/without a splitter plate rotated between 0° and 180° with 3° increments was tested at Re = 20000. Lift and drag force measurement was performed with the help of a load cell. The drag coefficient (C_D) is defined as $C_D = (2F_D)/\rho A u_\infty^2$, where F_D is the net drag force acting on the model, ρ is the density of air, A is the frontal area of the model based on D and V is the free stream velocity of air. The variation of drag coefficient as a function of attack angle for square cylinder with/without splitter plate is plotted in Figure 3. As expected, there is an axis of symmetry at 90° for the drag coefficient variation of the square cylinder without the plate. The drag coefficient significantly changes with an increasing attack angle. This change is attributed to the variation of flow structure with increasing attack angle. In the study of Sarioglu et al. (2006), the variation of drag and lift coefficients are shown in Figure 2 and 3 and are calculated from the integration of pressure measurements around the square prism. When C_D of the square cylinder is compared with the study of Sarioglu et al. (2006), C_D shows a similar trend as in this study. Their study neglect the pressure in the vicinity of square corners, therefore there is a little difference in the drag coefficient value. When results for the square cylinder with splitter plate at L/D = 1 are compared to the study of Sarioglu et al. (2006), the drag coefficients show substantial differences. Sarioglu et al. (2006), also did not consider the pressures acting on the splitter plate, even if it is of utmost importance. Therefore, C_D obtained from force measurements greatly differs from C_D obtained from pressure measurement. C_D is 2.02 for the square prism alone at α = 0°, 90° and 180°. When C_D found by the force measurement method is compared with values obtained by previous numerical and/or experimental studies, like the studies done by Shimada and Ishihara (2002), Sarioglu et al. (2006), Tamura and Miyagi (1999) and Lee (1975), C_D values are found to be in good agreement with this study at α = 0°. C_D values are also similar from α = 0° to α = 50° with values found by Sarioglu et al. (2006), Tamura and Miyagi (1999), Lee (1975).

C_D is 1.04 for the square prism with the splitter plate at α = 0°. The maximum drag reduction is 50% at 0°. This minimum drag is attributed to a base pressure increase with splitter plate as explained in study of Sarioglu et al. (2006). The drag coefficient decreases with increasing attack angle up to 15°. Due to the wide wake region with the plate at the downstream side, the highest value C_D = 2.26 occurs at α = 81°. For α < 30° and α > 114°, C_D values for a square prism together with the splitter plate are smaller than that of the square prism alone.

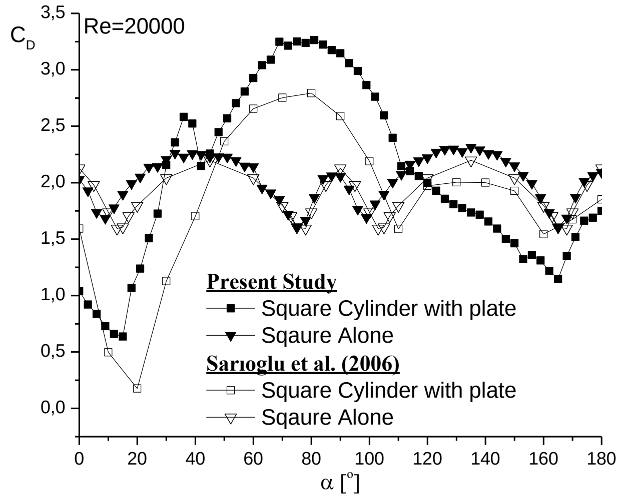

Figure3:

Variation of C_D with attack angle for square prism with/without plate

The lift coefficient (C_L) is defined as $C_L = (2F_L)/\rho A u_\infty^2$, where F_L is the net lift force acting on the model. C_L of the square prism with/without the plate for the present study and the study of Sarioglu et al. (2006) are shown in Figure 4 at Re = 20000. For the square cylinder alone, lift coefficient results of present study are in good agreement with that of the study of Sarioglu et al. (2006) except for 10°<α< 30° and 100°<α< 120°. Neglecting of the pressure on the splitter plate by Sarioglu et al. (2006), causes serious deviations of C_D as well as C_L as found by this study. The lift coefficient is near to zero at 0°, 90° and 180°. This can be attributed to the pressure balance between top and bottom side of the model. Variation of the lift coefficient with increasing attack angle from α = 0° to α = 50° shows an almost similar trend with Sarioglu et al. (2006), Tamura and Miyagi (1999) and Lee (1975). As shown in Figure 4, there is a significant change in lift coefficient with increasing attack angle for the square prism with/without splitter plate. Maximum C_L is obtained as 2.73 at 15° for the splitter plate case. The increase in C_L at this angle is associated to the reattachment of the separated shear layer.

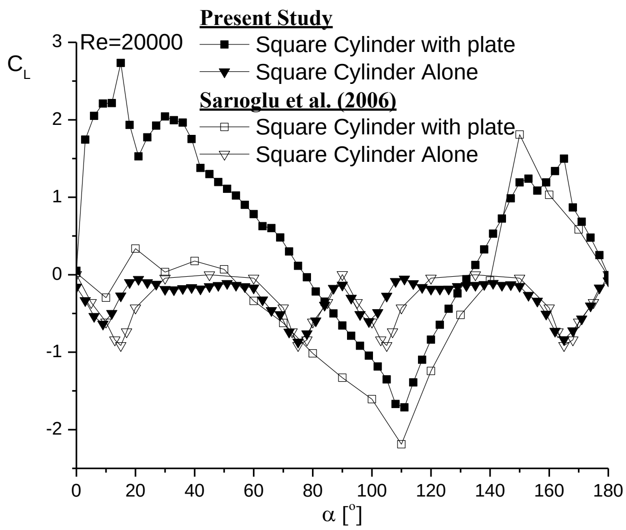

Figure4:

Variation of C_L with attack angle for square prism with/without plate

The effect of the Reynolds number on a square prism is investigated by measuring forces for Reynolds numbers ranging from 9700 to 36500 at different attack angles. Drag coefficient of both cases are plotted in Figure 5 at 0°, 45°, 90°, 135° and 180°.For all given attack angles, the drag coefficient for both cases are independent from the Reynolds number except for the case with a splitter plate at 0° and 90°.At these angles, the drag coefficient shows a slightly increasing trend with augmenting Reynolds numbers. Reynolds number independence implies that there is no change in the flow structure for these Reynolds numbers. Variation of attack angles leads to changes in the flow structure therefore C_D and C_L significantly change with an increasing attack angle.

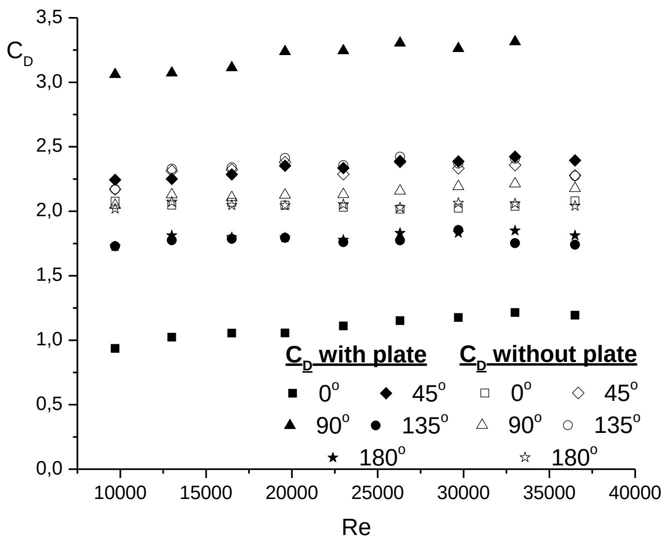

Figure 5:
Change in C_D with Reynolds number at incidence

The variation of C_L as a function of Reynolds number is given in Figure 6. The same experimental parameters are used as in the figure 5 plot. While lift coefficient is largely free of Reynolds number for the square cylinder alone at all given angles, it is not totally independent of Reynolds number for the square cylinder with splitter plate at 45°, 90° and 135° between Re = 9700 and 16500. At these angles and Reynolds range, there is a slight increase in the lift coefficient. Even so, it can be argued that C_L is largely independent of Reynolds number. While the flow structure changes with attack angle, it does not change by varying the Reynolds number.

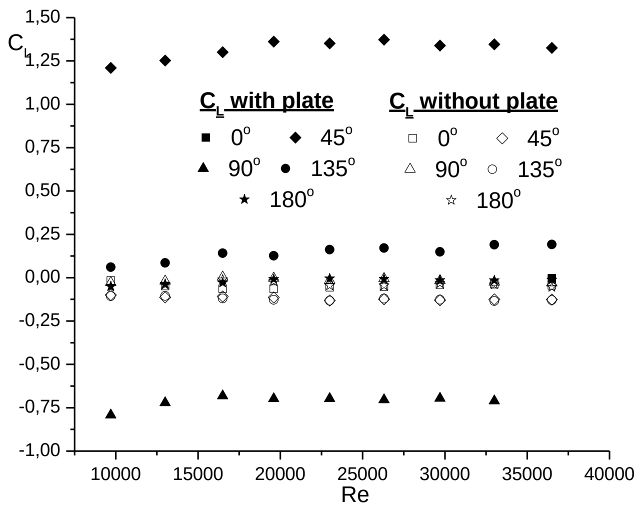

Figure6:
Change in C_L with Re at incidence

4. CONCLUSION

In this study, aerodynamic lift and drag forces acting on a square prism with or without a splitter plate is investigated by using a load cell at the attack angle range of 0° to 180° with 3° increments for Re = 20000. Experimental measurements were carried out to acquire knowledge on the effect of the Reynolds number by varying from Re = 9700 to 36500 at 0°, 45°, 90°, 135° and 180° attack angles. The results indicate that drag and lift coefficient is independent from Reynolds number in this region. Maximum drag reduction for the square cylinder with the plate is 50% as compared to the square cylinder alone at 0° and 15°. This present study also shows that, in the case of the square prism with an attached plate, force measurement with a load cell is better than calculating forces by using pressure measurements.

REFERENCES

1. Akansu, Y. E., Karakaya, F. and Şanlısoy, A. (2013) Active Control of Flow around NACA 0015 Airfoil by Using DBD Plasma Actuator, *EPJ Web of Conferences*, 45, 1008. doi:10.1051/epjconf/20134501008

2. Akansu, Y. E., Bayindirli, C. and Seyhan, M. (2016) The Improvement of Drag Force on a Truck Trailer Vehicle by Passıve Flow Control Methods. *Isı Bilimi ve Teknigi Dergisi-Journal of Thermal Science and Technology* 36(1):133–41.

3. Akansu, Y. E., Ozmert, M. and Firat, E. (2011) The Effect of Attack Angle to Vortex Shedding Phenomenon of Flow around a Square Prism with a Flow Control Rod, *Isı Bılımı Ve Teknıgı Dergısı-Journal Of Thermal Scıence And Technology*, 31(1), 109–120.

4. Akansu, Y. E., Sarioglu, M. and Yavuz, T. (2004) Flow around a Rotatable Circular Cylinder-Plate Body at Subcritical Reynolds Numbers, *AIAA Journal,* 42(6):1073–80. doi: 10.2514/1.4265.

5. Akbıyık, H., Yahya E. A., Yavuz, H. and Bay, A. E. (2016) Effect of Plasma Actuator and Splitter Plate on Drag Coefficient of a Circular Cylinder, *EPJ Web of Conferences*, 114, 1051. doi: 10.1051/epjconf/201611402001.

6. Bayındırlı, C. (2017) The Experimental Investigation of the Effects of Spoiler Design on Aerodynamic Drag Coefficient on Truck Trailer Combinations, *International Journal of Automotive Engineering and Technologies,* 6(0),11–18.

7. Bearman, P. W. and Harvey, J. K. (1993) Control of Circular Cylinder Flow by the Use of Dimples." *AIAA Journal* 31(10):1753–56. doi:10.2514/3.11844.

8. Coleman, H. W. and Steele, W. G. (2009) *Experimentation, Validation, and Uncertainty Analysis for Engineers*, John Wiley & Sons, New Jersey.

9. Fırat, E., Akansu, Y. E. and Akilli, H. (2015) Flow Past a Square Prism with an Upstream Control Rod at Incidence to Uniform Stream, *Ocean Engineering,* 108, 504–18. doi: 10.1016/j.oceaneng.2015.08.041.

10. Gilarranz, J. L., Traub, L. W. and Rediniotis, O. K. (2005) A New Class of Synthetic Jet Actuators—Part I: Design, Fabrication and Bench Top Characterization, *Journal of Fluids Engineering,* 127(2), 367-376. doi: 10.1115/1.1839931.

11. Godard, G. and Stanislas, M. (2006) Control of a Decelerating Boundary Layer. Part 1: Optimization of Passive Vortex Generators, *Aerospace Science and Technology* 10(3), 181–91. doi: 10.1016/j.ast.2005.11.007.

12. Lee, B. E. (1975) The Effect of Turbulence on the Surface Pressure Field of a Square Prism, *Journal of Fluid Mechanics*, 69(2), 263–82. doi:10.1017/S0022112075001437

13. Li, Z., Navon, I. M., Hussaini, M. Y. and Dimet, F. X. L. (2003) Optimal Control of Cylinder Wakes via Suction and Blowing, *Computers and Fluids*, 32(2), 149–171. doi: 10.1016/S0045-7930(02)00007-5

14. Vivek, M.and Oosthuizen. P. H. (1990) Effects of Splitter Plates on the Wake Flow behind a Bluff Body, *AIAA Journal*, 28(5), 778–83. doi:10.1016/S0045-7930(02)00007-5.

15. Rathakrishnan, E. (1999) Effect of Splitter Plate on Bluff Body Drag, *AIAA Journal*, 37(9), 1125–26. doi:10.2514/2.823.

16. Sarioglu, M. (2017) Control of Flow around a Square Cylinder at Incidence by Using a Splitter Plate, *Flow Measurement and Instrumentation*, 53, 221–29. doi:10.1016/j.flowmeasinst.2016.06.024.

17. Sarioglu, M., Akansu, Y. E. and Yavuz, T. (2006) Flow Around a Rotatable Square Cylinder-Plate Body, *AIAA Journal*, 44(5), 1065–72. doi:10.2514/1.18069.

18. Sarioglu, M., Akansu, Y. E. and Yavuz, T. (2005) Control of the Flow around Square Cylinders at Incidence by Using a Rod, *AIAA Journal*, 43(7), 1419–26. doi:10.2514/1.18069

19. Shimada, K. and Ishihara, T. (2002) Application of a Modified K–E Model to the Prediction of Aerodynamic Characteristics of Rectangular Cross-Section Cylinders, *Journal of Fluids and Structures*, 16(4), 465–85. doi:10.1006/jfls.2001.0433.

20. Tamura, T. and Miyagi, T. (1999) The Effect of Turbulence on Aerodynamic Forces on a Square Cylinder with Various Corner Shapes, *Journal of Wind Engineering and Industrial Aerodynamics*, 83(1), 135–45. doi:10.1016/S0167-6105(99)00067-7.

21. Volino, R. J. and Mounir B. I. (2012) Separation Control on High Lift Low-Pressure Turbine Airfoils Using Pulsed Vortex Generator Jets, *Applied Thermal Engineering*, 49, 31–40. doi:10.1016/j.applthermaleng.2011.08.028.

22. Zhang, Y. Y., Huang, D. G., Sun, X. J. and Wu, G. Q. (2010) Exploration in Optimal Design of an Airfoil with a Leading Edge Rotating Cylinder, *Journal of Thermal Science*, 19(4), 318–25. doi:10.1007/s11630-010-0389-6.